

Finding the center reliably: robust patterns of developmental gene expression

Martin Howard¹ and Pieter Rein ten Wolde²

¹*Department of Mathematics, Imperial College London,
South Kensington Campus, London SW7 2AZ, UK.*

²*FOM Institute for Atomic and Molecular Physics (AMOLF),
Kruislaan 407, 1098 SJ, Amsterdam, The Netherlands.*

(Dated: February 9, 2008)

We investigate a mechanism for the robust identification of the center of a developing biological system. We assume the existence of two morphogen gradients, an activator emanating from the anterior, and a co-repressor from the posterior. The co-repressor inhibits the action of the activator in switching on target genes. We apply this system to *Drosophila* embryos, where we predict the existence of a hitherto undetected posterior co-repressor. Using mathematical modelling, we show that a symmetric activator-co-repressor model can quantitatively explain the precise mid-embryo expression boundary of the *hunchback* gene, and the scaling of this pattern with embryo size.

PACS numbers: 87.18.La, 87.18.Bb, 05.40.-a

During embryonic development, cells have to differentiate in a manner that is dictated by their positions within the developing embryo. Turing conjectured that the positional information for differentiating cells is provided by molecules called morphogens that self-organize into spatial patterns [1]. Today a number of proteins have been identified that act as morphogens. However, in contrast to Turing's original conjecture, morphogens are usually produced at a localized source, after which they diffuse into the surrounding tissue. Here, morphogens are also degraded and a concentration gradient is thus formed. The differentiating cells respond via patterns of gene expression that depend on the morphogen concentration [2]. However, the biochemical processes that give rise to the morphogen gradient are prone to variations: the rates of protein synthesis/degradation, for example, will vary from embryo to embryo. Variation in these parameters might modify the morphogen gradient and thereby induce error in the positional information transmitted to the differentiating cells. Nevertheless, cell differentiation is often exceedingly precise [3]. How embryonic development is robust against fluctuations in the underlying biochemical processes is still poorly understood.

Recently, several mechanisms have been proposed to explain robust embryonic development [4, 5, 6]. They rely on the insensitivity of the morphogen gradient to embryo-to-embryo variations in the morphogen synthesis rates [4, 5, 6]. However, these mechanisms cannot explain recent experimental observations on the Bicoid-Hunchback system in the developing *Drosophila* embryo [3]. *bicoid* (*bcd*) messenger RNA (mRNA) is deposited at the anterior pole of the embryo, where it forms a localized source of Bcd protein. The Bcd protein diffuses away from the pole and is degraded, thereby forming a concentration gradient (see Fig.1a). A simple 'threshold' model would postulate that downstream genes such as *hunchback* (*hb*) are activated only when the concentration of Bcd is above a certain threshold [2].

However, while the *hb* expression domain is highly precise, the Bcd morphogen gradient exhibits large embryo-to-embryo variations [3, 7]. This rules out the above mechanisms, which rely on the robust formation of the morphogen gradient itself. Moreover, experiments reveal that the Hb boundary, x_{Hb} , scales with the embryo length (EL): $x_{\text{Hb}} = 0.49 (\pm 0.01) \text{ EL}$ [3]. Such scaling of expression domains cannot be explained by a single morphogen-gradient model, in which positional information is only emanating from one end. Indeed, this observation suggests that the formation of the *hb* expression domain is regulated by two or more morphogens, sourced at opposite ends of the embryo. Earlier work of Wolpert [2] and Meinhardt [8] already suggested that such models might provide size regulation.

Motivated by recent experimental observations [9, 10], which show that the activity of Bcd itself can be reduced by interactions with other proteins called co-repressors, we predict the existence of a second, as yet unidentified, morphogen that diffuses from a posterior-localized mRNA source. The co-repressor binds to Bcd, thereby inhibiting its ability to activate *hb* expression in the posterior half of the embryo (see Fig. 1a). We show that such a symmetric activator-co-repressor module can locate the embryo center reliably. Our model thus generates robust patterns of gene expression that scale with size, a result of potentially wide importance. Our calculations reveal that the module is highly robust against *correlated* embryo-to-embryo variations in the synthesis rates of the anterior activator (Bcd) and posterior co-repressor. Furthermore, variations in the synthesis rate of Bcd that are *uncorrelated* with that of the co-repressor, are also filtered far more than in a single-morphogen model. Identifying the proposed posterior morphogen may require a large-scale search for maternal mRNA localized to the posterior pole, which does not correspond to an already characterized maternal gene.

Mathematical Model. The outline of our model is

shown in Fig. 1: Bcd and co-repressor protein are injected at rates J_B , J_R at opposite ends of the embryo, where at each time instant the injection is concentrated at a randomly chosen location $x_B(t)$, $x_R(t)$ between $5\mu\text{m}$ and $30\mu\text{m}$ from the respective poles. The newly translated proteins diffuse away from the poles with diffusion constant D , and are degraded at a rate μ . Bcd and the co-repressor bind with rate ν to form a complex also with diffusion constant D . We assume that the reverse reaction occurs at a far slower rate, which we neglect. Only active Bcd (unbound to co-repressor) binds to the *hb* control region on the DNA to activate its transcription. Experiments suggest that this is a cooperative process [11], which we model with a Hill function with a coefficient of 3 [11]. However, the precise form of the activation function is not very important: taking other functional forms or changing the Hill coefficient to unity, for instance, does not alter our results, as the concentration of active Bcd is reduced to very low values at mid-embryo due to the co-repressor (see also below). Hb also auto-

activates its own synthesis via ‘synergistic’ interactions with (active) Bcd [3, 12]. *hb* mRNA has diffusion constant D_{hb} , and is spontaneously degraded with rate μ_{hb} . Hb protein is manufactured at a rate proportional to the mRNA concentration, has diffusion constant D_{Hb} and is spontaneously degraded with rate μ_{Hb} . These processes give the following equations, where $[B]$ is the unbound Bcd density, $[R]$ the co-repressor density, $[C]$ the Bcd-co-repressor complex density, $[hb]$ the *hb* mRNA density and $[Hb]$ the density of Hb protein:

$$\begin{aligned} \frac{\partial[B]}{\partial t} &= D \frac{\partial^2[B]}{\partial x^2} - \mu[B] - \nu[B][R] + J_B \delta(x - x_B(t)) \\ \frac{\partial[R]}{\partial t} &= D \frac{\partial^2[R]}{\partial x^2} - \mu[R] - \nu[B][R] + J_R \delta(x - x_R(t)) \\ \frac{\partial[C]}{\partial t} &= D \frac{\partial^2[C]}{\partial x^2} - \mu[C] + \nu[B][R] \\ \frac{\partial[hb]}{\partial t} &= D_{hb} \frac{\partial^2[hb]}{\partial x^2} - \mu_{hb}[hb] + \frac{\beta[B]^3(\eta[Hb] + \gamma K)}{K^4 + [B]^3(\eta[Hb] + K)} \\ \frac{\partial[Hb]}{\partial t} &= D_{Hb} \frac{\partial^2[Hb]}{\partial x^2} - \mu_{Hb}[Hb] + \alpha[hb]. \end{aligned}$$

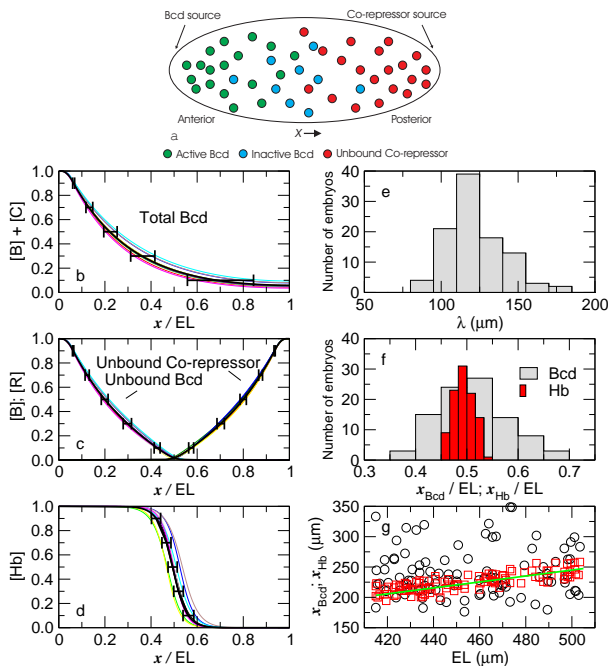


FIG. 1: a: Sketch of *Drosophila* embryo showing localized Bcd/co-repressor sources at opposite poles, and co-repressor-Bcd binding. b-g: Positional information for Bcd and Hb density profiles; data from 100 simulated embryos. Maximum densities normalized to unity. Mean density profile and standard deviation for: b: Total Bcd (Bcd plus complex); c: Unbound Bcd and co-repressor; d: Hb; in b)-d), 10 typical individual density profiles are also shown. e: Distribution of length scale λ describing exponential decay of total Bcd density profile. f: Distribution of positions x_{Bcd} and x_{Hb} where each Bcd and Hb density profile crosses given threshold, 0.17 for total Bcd, 0.5 for Hb. g: Positions x_{Bcd} and x_{Hb} as function of embryo length (EL); Bcd: circles, Hb: squares. Green straight line is $x_{Hb} = 0.49 \times EL$.

Here, we have used a simplified 1d model, where x measures the distance from the embryo’s anterior pole. Zero flux boundary conditions were imposed at both embryo ends. The wild-type parameters used were (see also [3]): $EL = 460\mu\text{m}$, $D = 10\mu\text{m}^2\text{s}^{-1}$, $D_{hb} = 0.5\mu\text{m}^2\text{s}^{-1}$, $D_{Hb} = 1\mu\text{m}^2\text{s}^{-1}$, $J_B = J_R = 0.08\text{s}^{-1}$, $\mu = 0.0007\text{s}^{-1}$, $\mu_{hb} = 0.004\text{s}^{-1}$, $\mu_{Hb} = 0.006\text{s}^{-1}$, $\nu = 3\mu\text{m}\text{s}^{-1}$, $\alpha = 0.006\text{s}^{-1}$, $\beta = 0.004\mu\text{m}^{-1}\text{s}^{-1}$, $\eta = 1.0$, $\gamma = 0.01$, $K = 0.045\mu\text{m}^{-1}$. We use the same diffusion constant/degradation rate for the complex as for unbound Bcd; this ensures that the total Bcd profile decays exponentially (as seen in experiment [3]), but is not important for the basic center finding properties of the model. Spatiotemporal fluctuations of the components within a single embryo, which could affect robustness [13], were also modelled but found to be less important than embryo-to-embryo variability and were therefore neglected. To simulate the embryo-to-embryo variability, the embryo length fluctuated by 10% [3]. Other parameters were varied by imposing a Gaussian distribution about the above average values, using the following standard deviation divided by the mean: $J_B : 0.05$, $J_R : 0.05$, $\mu : 0.3$, $\mu_{hb} : 0.3$, $\mu_{Hb} : 0.3$, $\alpha : 0.3$, $\beta : 0.3$, $K : 0.3$. The variations in the protein degradation rates were assumed to be correlated, while we studied both correlated and uncorrelated fluctuations in the Bcd and co-repressor source strengths. Initially, the system was empty of proteins and *hb* mRNA. The system reaches a steady state after ~ 1 hour, well before the window in which the relevant experiments were performed [3, 7].

It is conceivable that an additional activator [14] diffusing from the anterior competes with the co-repressor for Bcd binding. This, however, does not significantly change the results. Models in which the co-repressor and/or the Bcd-co-repressor complex can also bind to

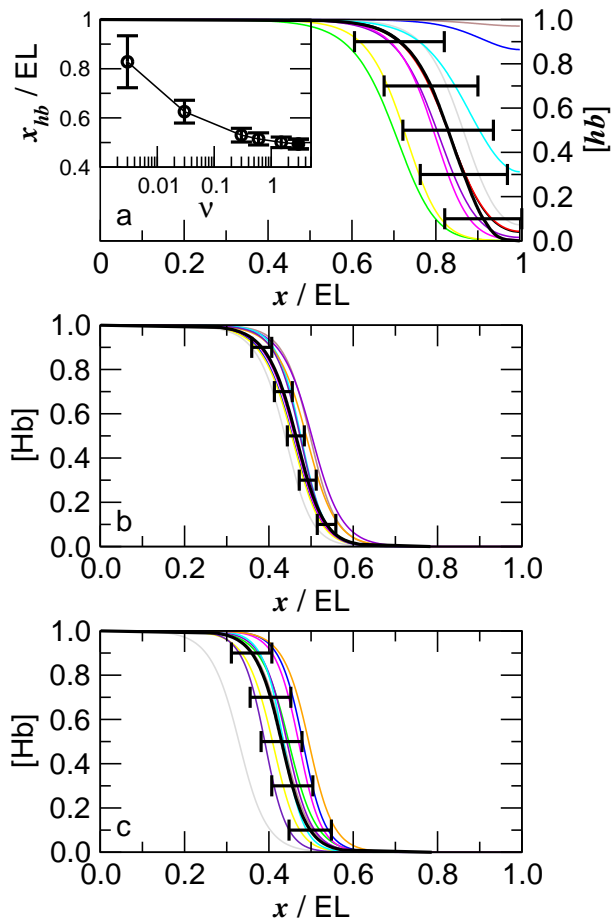


FIG. 2: a: *hb* mRNA profiles in simulated Bcd(A52-56) mutant ($\nu = 0.003\mu\text{ms}^{-1}$). Inset: mean/standard deviation for position of *hb* boundary as function of Bcd/co-repressor binding rate ν (closed symbol denotes wild type). b: Mean/standard deviation for Hb profile in mutant with malfunctioning Hb protein. c: Mean/standard deviation for Hb density profile in simulated *stauften* mutant (see text). Data from 100 simulated embryos; maximum densities normalized to unity; 10 typical individual profiles are also shown.

the DNA, but cannot then initiate *hb* transcription, again produce very similar results. Schemes in which Bcd and (co-)repressor *only* interact on the DNA, for instance by mutually excluding each other's DNA binding, provide scaling, but are less robust to variations in their parameters than the model proposed here. Furthermore, we have neglected the posterior morphogen *nanos* because if *nanos* is removed, the key properties of accuracy and scaling remain [3]. Lastly, while the co-repressor inactivates Bcd at mid-embryo with respect to *hb* expression, it does not impair Bcd's capacity to activate other genes in the embryo's posterior, such as *giant* and *knirps* [15]. Indeed, the Bcd domain that interacts with the co-repressor plays an inhibitory role in *hb* expression, but a positive role in *knirps* expression [16].

An alternative model has been suggested [17]; it assumes that the mRNA-localization protein Staufen trans-

ports *hb* mRNA away from the poles via a counter-intuitive mechanism relying on an *increased* diffusion rate of *hb* mRNA upon binding to Staufen. However, scaling is found over only 1-2 minutes rather than the required hour or more. Moreover, it predicts a gradient of Staufen, which is in contradiction with experiment [18]. Hence, as proposed here, a different mechanism may be needed.

Results. Simulation results of the above model, with uncorrelated fluctuations in the source strengths, are shown in Fig. 1. The density of Bcd plus Bcd-co-repressor complex decays exponentially away from the anterior pole (Fig. 1b), in agreement with experiment [3]. The total Bcd profile shows considerable embryo-to-embryo variation, with the characteristic length scale $\lambda = \sqrt{D/\mu}$ of the profile (Fig. 1e) and the position where the density crosses a threshold (Fig. 1f), both showing large fluctuations, similar to experiment [3, 7]. However, the profiles of the co-repressor/unbound Bcd fluctuate far less from embryo to embryo (Fig 1c); the fact that they bind, forces their unbound densities to very low values at mid-embryo. The active Bcd is then able to precisely activate *hb*: the *hb* mRNA (data not shown) and Hb protein (Fig. 1d) densities both pass their half-maximum values at x_{Hb} with little embryo-to-embryo variability, $x_{\text{Hb}} = 0.49(\pm 0.02)$ EL, see also Fig. 1f. The concentration profiles switch between their highest and lowest values over a length scale of about 0.1 EL. Both the average position and variation of the Hb boundary, as well as its steepness, are in agreement with experiment [3, 7]. Importantly, the Hb boundary location scales with the embryo size, unlike the Bcd profile [3, 7] (Fig. 1g). Furthermore, scaling is achieved even before the protein/mRNA concentrations reach steady-state, adding additional robustness to the model. Finally, scaling can be obtained even when the source strengths and λ are not the same for Bcd and co-repressor (data not shown).

A critical test of our model comes from varying the *bcd* gene dosage. When the dosage is halved (i.e. Bcd injection rate halved), the Hb boundary moves to $x_{\text{Hb}} = 0.39(\pm 0.02)$ EL. Simulations with twice and three times normal dosage, but assuming only 50% efficiency for the extra *bcd* genes as suggested by experiments [3, 10] (i.e. 1.5 and 2 times the wild type Bcd injection rate), move the boundary to $x_{\text{Hb}} = 0.56(\pm 0.025)$ EL and $x_{\text{Hb}} = 0.60(\pm 0.03)$ EL, respectively. Both the results on the mean and the variance agree with experiment [3]. Interestingly, the accuracy of *hb* expression is only weakly affected by changes in the *bcd* gene dosage: the standard deviation in x_{Hb} only increases by 50% when the Bcd injection rate changes from 0.5 to 2 times the wild type Bcd injection rate. More importantly, the average *hb* boundary moves by less than predicted by a simple threshold model [3]: the co-repressor gradient makes the boundary positioning more robust to variations in the protein production rates. Thus, the posterior morphogen not only provides scaling, but it also plays an important role as a

buffer against gene expression fluctuations.

Our model is also supported by several mutants. The Bcd(A52-56) mutant inhibits the ability of Bcd to interact with co-repressors [10]. We have modeled this by reducing the Bcd/co-repressor binding by a factor of 1000. Fig. 2a shows that this leads to a pronounced posterior shift in the *hb* expression pattern, in agreement with experiment [10]. We also predict that its precision will be lost: the *hb* boundary fluctuates strongly as the posterior co-repressor is no longer able to buffer against Bcd fluctuations. Experiments have also been performed in mutants that make detectable but malfunctioning Hb [3]. Normally Hb auto-activates its own synthesis [3, 12], and our model includes this effect. If, however, we assume that in this mutant Hb cannot stimulate its own synthesis (corresponding to $\eta = 0$), then the Hb boundary shifts anteriorly to $x_{\text{Hb}} = 0.46 (\pm 0.02)$ EL (Fig. 2b), while retaining its scaling properties. These results all accord with experiment [3, 12]. Further support comes from *stau*fen mutants. *Staufen* plays a central role in polar localizing maternal mRNAs [18, 19]. In the *stau*^{HL}/*stau*^{r9} mutants, the precision of the Hb boundary is lost and many of the Hb profiles are shifted anteriorly [3]. In contrast, the Bcd profile is not altered in the *stau*^{HL} mutants [3]. Taken together, these observations strongly suggest that in the *stau*^{HL}/*stau*^{r9} mutants, co-repressor mRNA is no longer properly localized at the posterior pole. We have studied this scenario by injecting a random fraction of the co-repressor close to the posterior (as described above), with the remainder randomly distributed throughout the embryo. The results are shown in Fig. 2c: Hb boundary precision is lost, and many profiles shift towards the anterior ($x_{\text{Hb}} = 0.43 (\pm 0.05)$ EL), in agreement with experiment [3].

To isolate which embryo-to-embryo variations are most

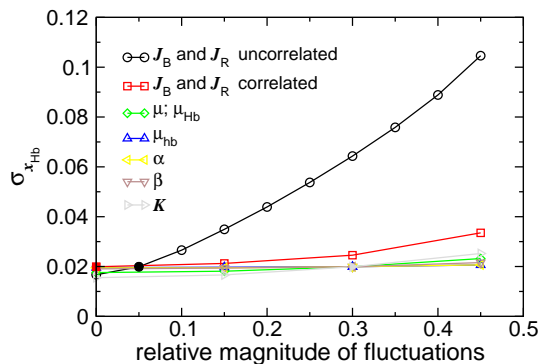


FIG. 3: Magnitude of variations in position of Hb boundary as a function of relative magnitude (standard deviation σ /mean value) of embryo-to-embryo variations in model parameters. Both uncorrelated and correlated variations in the injection rates J_B, J_R are shown (see text). When varying the fluctuations of one parameter, other parameters were fixed to their wild type values, indicated by closed symbols.

important, we studied the magnitude of the fluctuations

in the Hb boundary position as a function of the embryo-to-embryo variability of various parameters. Correlated variations that affect Bcd and the co-repressor similarly have little effect, due to the symmetry of the activator-co-repressor geometry (see Fig. 3). If, for instance, both Bcd and co-repressor are degraded by the same pathway, then the embryo-to-embryo variations in their degradation rates are correlated and thus filtered out (see Fig. 3). Furthermore, it is conceivable that not only degradation, but also synthesis of Bcd and co-repressor exhibit correlated embryo-to-embryo fluctuations, because they share, for instance, the same components of the transcription/translation apparatus. These correlated variations of the Bcd/co-repressor injection rates are again filtered (see Fig. 3). However, Bcd/co-repressor synthesis may also exhibit some uncorrelated variation. As we discussed above, our symmetric activator-co-repressor system buffers fluctuations far more than would be possible in a single morphogen system. Nevertheless, these uncorrelated fluctuations are not completely filtered out and, if large enough, can adversely affect the accurate positioning of the *hb* expression domain (see Fig. 3). Our model therefore predicts that Bcd synthesis must be tightly controlled, at least relative to that of the co-repressor.

We thank J. Ma, D. Bray, H. Bakker and M. Dogterom for comments and The Isaac Newton Institute for funding. MH acknowledges funding from The Royal Society. This work is part of the research program of FOM/NWO.

-
- [1] A. M. Turing, Phil. Trans. R. Soc. **B237**, 37 (1952).
 - [2] L. Wolpert, J. Theor. Biol. **25**, 1 (1969).
 - [3] B. Houchmandzadeh, E. Wieschaus, and S. Leibler, Nature **415**, 798 (2002).
 - [4] A. Eldar *et al.*, Nature **419**, 304 (2002).
 - [5] A. Eldar *et al.*, Dev. Cell **5**, 635 (2003).
 - [6] T. Bollenbach *et al.*, Phys. Rev. Lett. **94**, 018103 (2005).
 - [7] A. V. Spirov and D. M. Holloway, In Silico Biology **3**, 0009 (2003).
 - [8] H. Meinhardt, Development **104** Supplement, 95 (1988).
 - [9] W. Zhu *et al.*, Dev. Genes Evol. **211**, 109 (2001); C. Zhao *et al.*, J. Biol. Chem. **278**, 43901 (2003).
 - [10] C. Zhao *et al.*, Development **129**, 1669 (2002).
 - [11] X. Ma *et al.*, Development **122**, 1195 (1996); D. S. Burz *et al.*, EMBO J. **17**, 5998 (1998).
 - [12] M. Simpson-Brose, J. Treisman, and C. Desplan, Cell **78**, 855 (1994).
 - [13] J. L. England and J. Cardy, Phys. Rev. Lett. **94**, 078101 (2005).
 - [14] D. Fu, Y. Wen, and J. Ma, J. Biol. Chem. **279**, 48725 (2004).
 - [15] R. Rivera-Pomar *et al.*, Nature **376**, 253 (1995).
 - [16] D. Fu, C. Zhao, and J. Ma, Mol. Cell. Biol. **23**, 4439 (2003).
 - [17] T. Aegerter-Wilmsen, C. M. Aegerter, and T. Bisseling, J. Theor. Biol. **234**, 13 (2005).
 - [18] D. St Johnston, D. Beuchle, and C. Nüsslein-Volhard, Cell **66**, 51 (1991).
 - [19] D. Ferrandon *et al.*, Cell **79**, 1221 (1994).